

A chiral symmetric relativistic mean field model with logarithmic sigma potential^{*)}

Kohsuke TSUBAKIHARA and Akira OHNISHI

*Department of Physics, Faculty of Science, Hokkaido University,
Sapporo 060-0810, Japan*

We develop a chiral symmetric relativistic mean field model with logarithmic sigma potential derived in the strong coupling limit of the lattice QCD. We find that both of nuclear matter and finite nuclei are well described in the present model. The normal vacuum is found to have global stability at zero and finite baryon densities, and an equation of state with moderate stiffness ($K \simeq 280$ MeV) is obtained. Binding energies and charge radii of Z closed even-even nuclei are well reproduced in a wide mass range from C to Pb isotopes, except for the underestimates of binding energies in several jj closed nuclei.

§1. Introduction

Chiral symmetry is a fundamental symmetry of QCD at zero quark masses, and its spontaneous symmetry breaking generates constituent quark and hadron masses. The Nambu-Goldstone boson of chiral symmetry, *i.e.* pion, mediates the long range part of nuclear force,¹⁾ and the midrange attractive nuclear force can be described with a light scalar isoscalar meson, so called σ , which would be the chiral partner of the pion and represent the fluctuation of the chiral condensate. Thus it is desirable to respect chiral symmetry in theories of quark, hadron, and nuclear physics. Actually, many models and theories of quarks and hadrons such as the sigma model,²⁾ the Nambu-Jona-Lasino model,^{3),4)} and the chiral perturbation theories⁵⁾ have been constructed on the basis of chiral symmetry.

In nuclear many-body problems, relativistic mean field (RMF) models have been developed to describe properties of nuclear matter and finite nuclei. The first RMF model proposed by Serot and Walecka⁶⁾ includes sigma and omega (isoscalar vector) mesons and their linear couplings to nucleons. Later on, non-linear self-coupling terms of sigma⁷⁾⁻¹⁰⁾ and omega mesons^{10),11)} are introduced to obtain better descriptions of nuclear matter and finite nuclei. These Lagrangians contain $\sigma^2, \sigma^3, \sigma^4$ terms, which remind us of the chiral linear σ model Lagrangian. RMF models have been successfully applied to various nuclear many-body problems; nuclear matter saturation,⁶⁾ single particle levels in finite nuclei including the spin-orbit splittings,⁶⁾ nuclear binding energies,⁸⁾⁻¹⁰⁾ nucleon-nucleus scatterings,¹²⁾ and compact astrophysical objects such as neutron stars and supernovae.¹³⁾⁻¹⁵⁾ Having these successes and the Lagrangian forms in mind, it is natural to expect that RMF is not only a phenomenological model parameterizing nuclear energy functionals, but also a starting point of finite baryon density hadronic models provided that chiral symmetry is respected.

^{*)} Prog. Theor. Phys. (2007), in press [arXiv: nucl-th/0607046].

Contrary to the expectations above, simple chiral RMF models fail to describe nuclei as nucleon many-body systems. Since the valence nucleon Fermi integral prefers smaller chiral condensate, the normal vacuum jumps to a chiral restored abnormal one (so-called *chiral collapse*¹⁶⁾) below the normal nuclear density in a mean field treatment of the linear σ model.^{17)–19)} In order to solve this problem, several prescriptions have been proposed to generate additional repulsive potential at small σ values, where $\sigma \propto -\langle \bar{q}q \rangle$. One of the prescriptions is to include fermion loop effects.^{19)–21)} In the baryon one-loop renormalization, non-linear and non-analytic sigma potential terms appear and stabilize the normal vacuum.^{19),20)} Similar terms are obtained from quark loops,⁴⁾ and it is possible to suppress the chiral collapse and to reproduce the saturation point by tuning the coefficients of these terms.²¹⁾ In both of the cases, instability at large σ values is caused by the generated interaction term, $-\sigma^4 \log \sigma^2$. In addition, meson loops generally cancel a large part of additional repulsion from fermion loops,^{22),23)} then the chiral collapse problem remains. The second approach is to introduce the coupling of sigma and omega mesons.^{18),24)} The partial chiral symmetry restoration reduces omega meson mass and enhances the repulsive vector interaction, then the normal vacuum is kept stable even at high densities. Quantitatively, however, repulsive vector interaction becomes so large that the nuclear matter is found to be very stiff.^{18),24)} It is possible to soften the EOS by including higher order terms such as σ^6 and σ^8 , but these terms cause instability at large σ values.²⁵⁾

The third way to overcome the chiral collapse problem is to incorporate the glueball field which simulates the scale anomaly in QCD.^{26)–31)} While it may not be justified to include the unobserved glueballs in hadronic models, these models give nuclear matter incompressibility in an acceptable range, and they roughly explain the bulk properties of nuclei.²⁷⁾ From the symmetry requirement, the glueball is conjectured to couple with σ in the form of $-\chi^4 \log \sigma^2$, where χ denotes the glueball field. This potential term ensures the stability of the normal vacuum in the mean field approximation. The mass of the glueball is assumed to be heavy, 1 – 2 GeV, then it would be reasonable to consider the glueball expectation value as constant in low energy phenomena.²⁷⁾ Under this assumption, the above potential term is divergent at $\sigma \rightarrow 0$ and keeps the normal vacuum stable.

These approaches are based on QCD inspired effective models, and it is preferable to obtain the chiral potential (energy density as a function of σ) directly from QCD. At present, it is not yet possible to obtain the chiral potential in Monte-Carlo simulations of the lattice QCD, since the quark loop contribution is very strong in the chiral (massless) limit. One of the promising directions would be to invoke the strong coupling limit of the lattice QCD (SCL-LQCD). Actually, a logarithmic σ potential term similar to that in the glueball model was already derived.³²⁾ In SCL-LQCD, the pure gluonic action disappears and we can perform the one-link integral,^{32)–37)} then we can obtain an analytic expression of the chiral potential with a logarithmic term, $-\log \sigma^2$.^{32),33)}

In this paper, we study nuclear matter and finite nuclei in a flavor SU(2) chiral symmetric relativistic mean field model containing the logarithmic chiral potential term, $-\log \sigma^2$, derived from SCL-LQCD^{32),33)} in vacuum. We also include vec-

tor mesons (ω, ρ), their linear couplings to nucleons, and ω self-interaction term, $(\omega_\mu \omega^\mu)^2$, in the effective Lagrangian phenomenologically. Requiring that the pion and nucleon masses and the pion decay constant are given, we have four free parameters, $m_\sigma, g_\omega, g_\rho$ and c_ω (σ mass, coupling constants of nucleons with ω and ρ mesons, and the coefficient of the $(\omega_\mu \omega^\mu)^2$ term). Two of these parameters (g_ω and c_ω) are determined to fit the nuclear matter saturation point, $(\rho_0, E/A) = (0.145 \text{ fm}^{-3}, -16.3 \text{ MeV})$, and the others (m_σ and g_ρ) are determined to reproduce the binding energies of Sn and Pb isotopes. By choosing these parameters appropriately, we find that the obtained EOS is as soft as those in other successful RMF models such as NL3 and TM1 models.^{9),10)} Bulk properties (binding energies and charge radii) of proton (sub-)closed even-even nuclei are also well explained in a comparable precision to NL1,⁸⁾ NL3,⁹⁾ and TM1¹⁰⁾ models.

We consider a linear $N\sigma$ coupling in this paper, where the nucleon mass is a linear function of σ . When the quark structure of nucleons are considered, we may have non-linear $N\sigma$ couplings.^{38)–40)} Based on the MIT bag model³⁸⁾ or the NJL model,³⁹⁾ it is demonstrated that the nucleon mass can have a curvature as a function of σ , known as the scalar polarizability. This positive curvature leads to a repulsion between the nucleons, which prevents the chiral collapse.^{38),39)} The non-linear $N\sigma$ coupling and the chiral potential have to be considered simultaneously. We discuss this point in Sec. 4.

There are several works including the negative parity baryons^{21),41)} and works based on another chiral partner assignment of pions.⁴²⁾ While these are promising approaches, we stick to a naive assignment of nucleon and pion chiral partners in this work. Finite temperature and finite chemical potential treatments in SCL-LQCD^{33)–37)} would be also necessary to describe the chiral phase transition at high temperatures and densities, but these are beyond the scope of this paper.

This paper is organized as follows. In Sec. 2, we briefly explain the derivation of the chiral potential in SCL-LQCD, and describe our effective hadronic Lagrangian. In Sec. 3, we discuss the properties of nuclear matter and finite nuclear properties in the present model in comparison with other models. In Sec. 4, we examine the naturalness of the obtained effective Lagrangian through the naive dimensional analysis (NDA),^{29),40),43)} and we also interpret the present Lagrangian in terms of the scalar polarizability.³⁸⁾ We summarize our work in Sec. 5.

§2. Chiral symmetric sigma potential

2.1. Logarithmic chiral potential in the strong coupling limit of the lattice QCD

Chiral potential V_σ (energy density as a function of σ in vacuum) is one of the most important ingredients in chiral models. In this paper, we utilize the chiral potential derived in the strong coupling limit of the lattice QCD (SCL-LQCD).^{32)–34)} Here we briefly summarize how to derive the chiral potential. Detailed derivations are found in Refs. 32)–34).

In SCL ($g_{\text{QCD}} \rightarrow \infty$), we can ignore the pure gluonic part of the lattice action

which is proportional to $1/g_{QCD}^2$, and we keep only those terms including fermions,

$$S_F[\chi, \bar{\chi}, U] = \frac{1}{2} \sum_{x, \mu} \eta_\mu(x) \left[\bar{\chi}(x) U_\mu(x) \chi(x + \hat{\mu}) - \bar{\chi}(x + \hat{\mu}) U_\mu^\dagger(x) \chi(x) \right], \quad (2.1)$$

where $\eta_\mu(x) = (-1)^{x_0+x_1+\dots+x_{\mu-1}}$, and we express the action in the lattice unit. We consider two species of staggered fermions simulating u and d quarks. After integrating out the link variable U_μ in the leading order of $1/d$ expansion and introducing the auxiliary fields $\sigma_{\alpha\beta}$, we obtain the following partition function,

$$\begin{aligned} \mathcal{Z} &= \int \mathcal{D}[\chi, \bar{\chi}, U] \exp(-S_F[\chi, \bar{\chi}, U]) \\ &\simeq \int \mathcal{D}[\chi, \bar{\chi}] \exp \left[\frac{1}{2} \sum_{x, y, \alpha, \beta} \mathcal{M}_{\alpha\beta}(x) V_M(x, y) \mathcal{M}(y)_{\beta\alpha} \right] \\ &= \int \mathcal{D}[\chi, \bar{\chi}, \sigma] \exp(-S_\sigma[\chi, \bar{\chi}, \sigma]), \end{aligned} \quad (2.2)$$

$$S_\sigma[\chi, \bar{\chi}, \sigma] = \sum_{x, y, \alpha, \beta} \left[\frac{1}{2} \sigma(x)_{\alpha\beta} V_M(x, y) \sigma(y)_{\beta\alpha} + \sigma(x)_{\alpha\beta} V_M(x, y) \mathcal{M}(y)_{\beta\alpha} \right]. \quad (2.3)$$

Mesonic composites are defined as $\mathcal{M}_{\alpha\beta}(x) = \bar{\chi}_\alpha^a(x) \chi_\beta^a(x)$, where a denotes color, and α and β show the flavor. The lattice mesonic inverse propagator $V_M(x, y)$ is given as $V_M(x, y) = \sum_\mu (\delta_{y, x+\hat{\mu}} + \delta_{y, x-\hat{\mu}}) / 4N_c$. From the first to the second line in Eq. (2.2), we have used the one-link integral formula, $\int dU U_{ab} U_{cd}^\dagger = \delta_{ad} \delta_{bc} / N_c$. The auxiliary fields are related to the expectation values of the mesonic composites as $\langle \sigma_{\alpha\beta}(x) \rangle = -\langle \mathcal{M}_{\alpha\beta}(x) \rangle$.

Now we consider static and uniform scalar σ and pseudoscalar $\boldsymbol{\pi}$ condensates, and we substitute the auxiliary fields by the mean field ansatz, $\sigma_{\alpha\beta}(x) = s(\sigma + i\varepsilon(x) \boldsymbol{\tau} \cdot \boldsymbol{\pi})_{\alpha\beta} / \sqrt{2}$, where $\varepsilon(x) = (-1)^{x_0+x_1+x_2+x_3}$ and s is a scaling factor to connect the chiral condensate and physical σ and $\boldsymbol{\pi}$ fields. Since fermions are decoupled in each space-time point, we can easily perform the fermion integral. The chiral potential is obtained in the lattice unit as,

$$\begin{aligned} V_\chi(\sigma, \boldsymbol{\pi}) &= \frac{1}{2} \langle \sigma_{\alpha\beta} V_M \sigma_{\beta\alpha} \rangle - N_c \log \det [\sigma_{\alpha\beta} V_M] \\ &= \frac{s^2}{2} \langle V_M \rangle \text{tr} [M^\dagger M] - N_c \log \det M \\ &= \frac{1}{2} b_\sigma \phi^2 - a_\sigma \log \phi^2, \end{aligned} \quad (2.4)$$

$$\phi^2 = \sigma^2 + \boldsymbol{\pi}^2, \quad a_\sigma = \frac{N_c}{a_{\text{lattice}}^4}, \quad b_\sigma = \frac{d+1}{2N_c} s^2 a_{\text{lattice}}^2, \quad (2.5)$$

where $\langle \dots \rangle$ denotes the space-time average, and $d=3$ is the spatial dimension. The meson matrix M is given as $M = (\sigma + i\boldsymbol{\tau} \cdot \boldsymbol{\pi}) / \sqrt{2}$. In Eq. (2.5), we explicitly write the lattice spacing a_{lattice} .

With an explicit symmetry breaking term, we require that physical masses of σ and π mesons are obtained in the mean field approximation.

$$V_\sigma^{\text{SCL}} = V_\chi(\sigma, \boldsymbol{\pi}) - c_\sigma \sigma = \frac{1}{2} b_\sigma \phi^2 - a_\sigma \log \phi^2 - c_\sigma \sigma \quad (2.6)$$

$$= \frac{1}{2} m_\sigma^2 \varphi^2 + \frac{1}{2} m_\pi^2 \boldsymbol{\pi}^2 + \mathcal{O}((\varphi, \boldsymbol{\pi})^3) \quad (\varphi = f_\pi - \sigma). \quad (2.7)$$

After fitting the vacuum equilibrium value $\sigma = f_\pi$ and the pion mass m_π , parameters $a_\sigma, b_\sigma, c_\sigma$ are represented with one parameter m_σ , which is treated as a free parameter,

$$a_\sigma = \frac{f_\pi^2}{4} (m_\sigma^2 - m_\pi^2), \quad b_\sigma = \frac{1}{2} (m_\sigma^2 + m_\pi^2), \quad c_\sigma = f_\pi m_\pi^2. \quad (2.8)$$

In a present context, one can think that this procedure is equivalent to tune the lattice spacing and the scaling factor in Eq. (2.5). However, the coefficients a_σ and b_σ in Eq. (2.5) depend on the details of the derivation. For example, it has been shown that the baryonic composite contribution modifies the coefficient b_σ .³³⁾ Furthermore, two species of staggered fermions correspond to $N_f = 8$, and the coefficient modification may not be trivial when we take $N_f = 2$. Thus we regard them as parameters to obtain physical masses of σ and π mesons in the mean field approximation.

Because of the singularity of V_σ at $\sigma \rightarrow 0$, chiral symmetry restoration is suppressed with this chiral potential. One can doubt that this singularity may come from an artifact of SCL-LQCD. Indeed, in a finite temperature treatment of SCL-LQCD, we do not have a divergent behavior at $\sigma \rightarrow 0$,³³⁾⁻³⁶⁾ but we still have a finite negative derivative at $\sigma \rightarrow 0$ in cold matter ($T = 0$). This finite negative derivative at $\sigma = 0$ is enough to suppress the full chiral restoration at finite density, because the nucleon Fermi integral contribution behaves as $\rho_B \sigma^2$ and we always have a minimum at a finite σ value. Therefore, we consider that the present chiral potential V_σ would be a good starting point to describe cold nuclear matter and nuclei. At finite temperatures, the singularity disappears also in the derivative, and the full chiral restoration will take place in SCL-LQCD.³³⁾⁻³⁶⁾ In that case, we have to take account of the finite temperature effects in V_σ .

2.2. Comparison with other models

There is a variety of chiral potentials proposed so far. The simplest one is found in the chiral linear σ model (ϕ^4 theory) proposed by Gell-Mann and Levy,²⁾

$$V_\sigma^{(\phi^4)} = \frac{\lambda}{4} (\phi^2 - f_\pi^2)^2 + \frac{1}{2} m_\pi^2 \phi^2 - f_\pi m_\pi^2 \sigma, \quad \lambda = \frac{m_\sigma^2 - m_\pi^2}{2f_\pi^2}, \quad (2.9)$$

where we have only one free parameter m_σ and the theory is renormalizable. In the Nambu-Jona-Lasino(NJL) model,^{3),4)} the chiral symmetric four quark interaction dynamically breaks chiral symmetry and generates the chiral potential having a wine bottle structure. The chiral potential in NJL is found to be

$$V_\sigma^{\text{NJL}} = \frac{m_0^2}{2} \sigma^2 + \Lambda^4 f_{\text{NJL}} \left(\frac{G\sigma}{\Lambda} \right) - f_\pi m_\pi^2 \sigma, \quad (2.10)$$

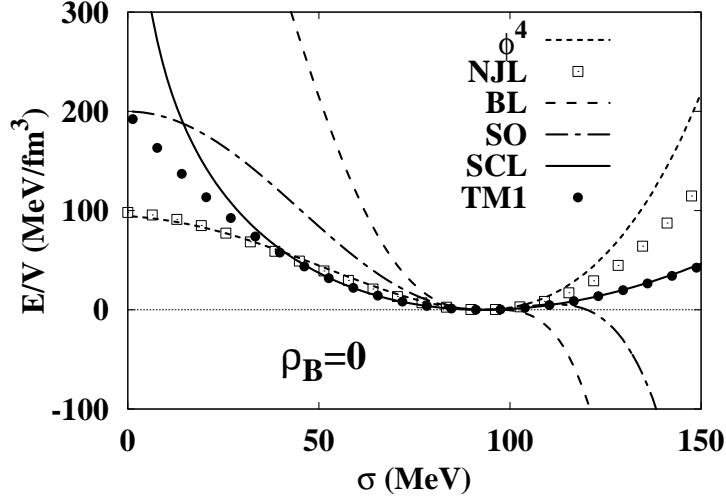


Fig. 1. Energy density in vacuum as a function of σ in the SCL model (solid curve) is compared with those in the linear σ (ϕ^4 , dotted curve), NJL^{3),4)} (open squares), baryon loop (BL, dashed lines)²⁰⁾, Sahu-Ohnishi (SO, dot-dashed lines)²⁵⁾, and TM1 (filled circles)¹⁰⁾ models.

$$f_{\text{NJL}}(x) = -\frac{N_c N_f}{4\pi^2} \left[\left(1 + \frac{x^2}{2}\right) \sqrt{1+x^2} - 1 - \frac{x^4}{2} \log \left(\frac{1 + \sqrt{1+x^2}}{x} \right) \right], \quad (2.11)$$

where G represents the coupling of the quark to σ and π mesons.⁴⁾ In Ref. 4), parameter values are fixed to fit f_π and m_π , resulting in the constituent quark mass $M_q = Gf_\pi = 335$ MeV and cut off $\Lambda = 631$ MeV.

Nucleon one-loop renormalization in the chiral linear σ model leads to additional potential terms in vacuum. In the chiral limit ($m_\pi = 0$), the following interaction appears,²⁰⁾

$$V_\sigma^{\text{BL}} = \frac{m_\sigma^2}{8f_\pi^2} (\phi^2 - f_\pi^2)^2 - M_N^4 f_{\text{BL}}(\phi/f_\pi), \quad (2.12)$$

$$f_{\text{BL}}(x) = -\frac{1}{4\pi^2} \left[\frac{x^4}{2} \log x^2 - \frac{1}{4} + x^2 - \frac{3}{4}x^4 \right]. \quad (2.13)$$

In Ref. 20), the value of sigma mass is taken to be $m_\sigma = 572.8$ MeV.

In order to obtain reasonable incompressibility within the Boguta scenario,¹⁸⁾ it is proposed to add higher order terms,²⁵⁾ and their chiral potential is given in the chiral limit as follows,

$$V_\sigma^{\text{SO}} = \frac{m_\sigma^2}{8f_\pi^2} (\phi^2 - f_\pi^2)^2 + f_\pi^4 f_{\text{SO}}(\phi/f_\pi), \quad (2.14)$$

$$f_{\text{SO}}(x) = \frac{C_6}{6} (x^2 - 1)^3 + \frac{C_8}{8} (x^2 - 1)^4, \quad (2.15)$$

with parameters $m_\sigma = 762.3$ MeV, $C_6 = -74.4$ and $C_8 = -2.2$.

For comparison, we also refer here the potential in a non-chiral model, TM1.¹⁰⁾

$$V_{\sigma}^{\text{TM1}}(\varphi) = \frac{m_{\sigma}^2}{2}\varphi^2 + \frac{g_3 f_{\pi}}{3}\varphi^3 + \frac{g_4}{4}\varphi^4, \quad (2.16)$$

where φ stands for the deviation from the vacuum, $\varphi = f_{\pi} - \sigma$. Parameters in the TM1 model are given as $m_{\sigma} = 511.198$ MeV, $g_3 = 15.3383$ and $g_4 = 0.6183$.

In Fig. 1, we compare the chiral potential in the present SCL model, V_{σ}^{SCL} in Eq. (2.6), with those in other models. The chiral potential in the NJL model agrees with that in the linear σ model (ϕ^4) in the region $\sigma < f_{\pi}$. As mentioned in the introduction, the nucleon Fermi contribution prefers smaller σ values at finite density, and in order to keep σ from collapsing at finite densities, we need more repulsive potential at small σ values. While the repulsion is enough to prevent this collapse in the baryon loop (BL) and Sahu-Ohnishi (SO) models, these models have instability at large σ . In the present SCL model, there is no instability, and strong repulsion at small σ suppresses the chiral collapse. It is interesting to find that the SCL model result is very close to that in the TM1 except for the divergent behavior at $\sigma \rightarrow 0$.

§3. Nuclear matter and finite nuclei in chiral RMF models

RMF approach has been developed as an effective theory to describe nuclear matter and finite nuclei in a field theoretical treatment. In this paper, we consider the following chiral symmetric RMF Lagrangian in which nucleons couple with σ , $\boldsymbol{\pi}$, ω and $\boldsymbol{\rho}$ fields,

$$\begin{aligned} \mathcal{L}_{\chi} = & \bar{\psi}_N [i\cancel{\partial} - g_{\sigma}(\sigma + i\gamma_5 \boldsymbol{\tau} \cdot \boldsymbol{\pi}) - g_{\omega}\cancel{\omega} - g_{\rho}\boldsymbol{\tau} \cdot \boldsymbol{\rho}] \psi_N \\ & + \frac{1}{2}(\partial^{\mu}\sigma\partial_{\mu}\sigma + \partial^{\mu}\boldsymbol{\pi} \cdot \partial_{\mu}\boldsymbol{\pi}) - V_{\sigma}(\sigma, \boldsymbol{\pi}) \\ & - \frac{1}{4}W^{\mu\nu}W_{\mu\nu} + \frac{1}{2}m_{\omega}^2\omega^{\mu}\omega_{\mu} + \frac{c_{\omega}}{4}(\omega^{\mu}\omega_{\mu})^2 - \frac{1}{4}\mathbf{R}^{\mu\nu} \cdot \mathbf{R}_{\mu\nu} + \frac{1}{2}m_{\rho}^2\boldsymbol{\rho}^{\mu} \cdot \boldsymbol{\rho}_{\mu}, \end{aligned} \quad (3.1)$$

$$W_{\mu\nu} = \partial_{\mu}\omega_{\nu} - \partial_{\nu}\omega_{\mu}, \quad (3.2)$$

$$\mathbf{R}_{\mu\nu} = \partial_{\mu}\boldsymbol{\rho}_{\nu} - \partial_{\nu}\boldsymbol{\rho}_{\mu} + g_{\rho}\boldsymbol{\rho}_{\mu} \times \boldsymbol{\rho}_{\nu}. \quad (3.3)$$

Here we have omitted the photon field and we include that for finite nuclear studies.

In this section, we study uniform nuclear matter and finite nuclei with the Lagrangian in Eq. (3.1) by using the logarithmic chiral potential V_{σ}^{SCL} in Eq. (2.6). We search for an appropriate parameter set, containing the σ mass (m_{σ}), meson-nucleon coupling constants (g_{ω} and g_{ρ}), and the strength of the ω self-interaction (c_{ω}), which explains the properties of symmetric nuclear matter and finite nuclei.

3.1. Nuclear Matter

First, we study the EOS of uniform symmetric nuclear matter. We assume that the meson fields are static and uniform, then the RMF Lagrangian for nuclear matter becomes

$$\mathcal{L}_{\chi}^{\text{Unif}} = \bar{\psi}_N (i\cancel{\partial} - g_{\sigma}\sigma - \gamma^0(g_{\omega}\omega + g_{\rho}\tau_3 R)) \psi_N$$

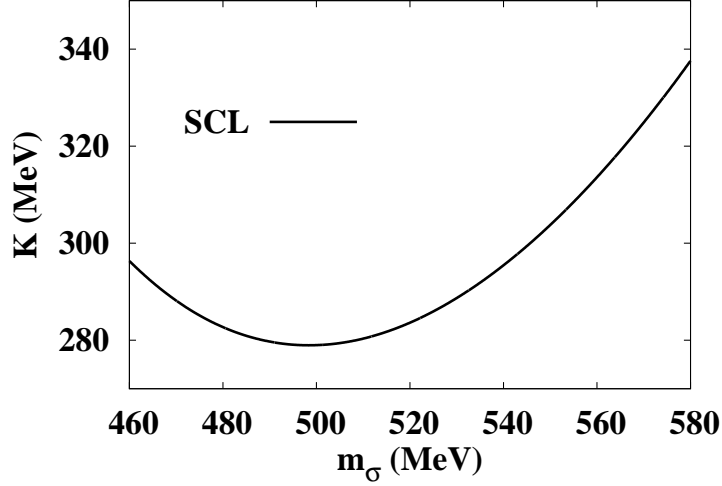


Fig. 2. Symmetric nuclear matter incompressibility K as a function of σ mass (m_σ) in the SCL model. For a given m_σ value, the ω -nucleon coupling constant (g_ω) and the ω self-interaction strength (c_ω) are determined to fit the symmetric nuclear matter saturation point, $(\rho_0, E/A)$, and the incompressibility K is obtained as a result of fitting.

$$+\frac{1}{2}m_\omega^2\omega^2 + \frac{c_\omega}{4}\omega^4 + \frac{1}{2}m_\rho^2R^2 - V_\sigma(\sigma) , \quad (3.4)$$

which includes σ , ω and ρ (written as R) mesons. Here we have omitted the Lorentz and isospin indices, $\omega = \omega_0$ and $R = \rho_{30}$, for simplicity.

The energy density in symmetric nuclear matter can be written as,

$$E/V = g_N \int^{p_F} \frac{d\mathbf{p}}{(2\pi)^3} \sqrt{p^2 + M_N^{*2}(\sigma)} + g_\omega\omega\rho_B - \frac{m_\omega^2}{2}\omega^2 - \frac{c_\omega}{4}\omega^4 + V_\sigma(\sigma) , \quad (3.5)$$

where $g_N = 4$ is the nuclear spin-isospin degeneracy, and $M_N^*(\sigma) = g_\sigma\sigma$ is the nucleon effective mass. The equilibrium conditions read

$$\frac{\partial(E/V)}{\partial\sigma} = g_\sigma\rho_s + \frac{\partial V_\sigma}{\partial\sigma} = 0 , \quad \rho_s = g_N \int^{p_F} \frac{d\mathbf{p}}{(2\pi)^3} \frac{M_N^*(\sigma)}{\sqrt{p^2 + M_N^{*2}(\sigma)}} , \quad (3.6)$$

$$\frac{\partial(E/V)}{\partial\omega} = g_\omega\rho_B - m_\omega^2\omega - c_\omega\omega^3 = 0 . \quad (3.7)$$

In symmetric nuclear matter, we have three relevant parameters, m_σ , g_ω and c_ω . When we give m_σ as a free parameter, then other two are determined to fit the saturation properties, $(\rho_0, E/A) = (0.145 \text{ fm}^{-3}, -16.3 \text{ MeV})$. In Fig. 2, we show the nuclear matter incompressibility $K = 9\rho_0^2(\partial^2(E/V)/\partial\rho_B^2)$ as a function of m_σ . We find that the incompressibility is smaller than 300 MeV in the mass region $460 \text{ MeV} \lesssim m_\sigma \lesssim 540 \text{ MeV}$, which can be regarded as the allowed region. Especially, at around the incompressibility minimum ($K \simeq 279 \text{ MeV}$ at $m_\sigma \sim 500 \text{ MeV}$), we obtain EOS as soft as that in TM1.¹⁰⁾

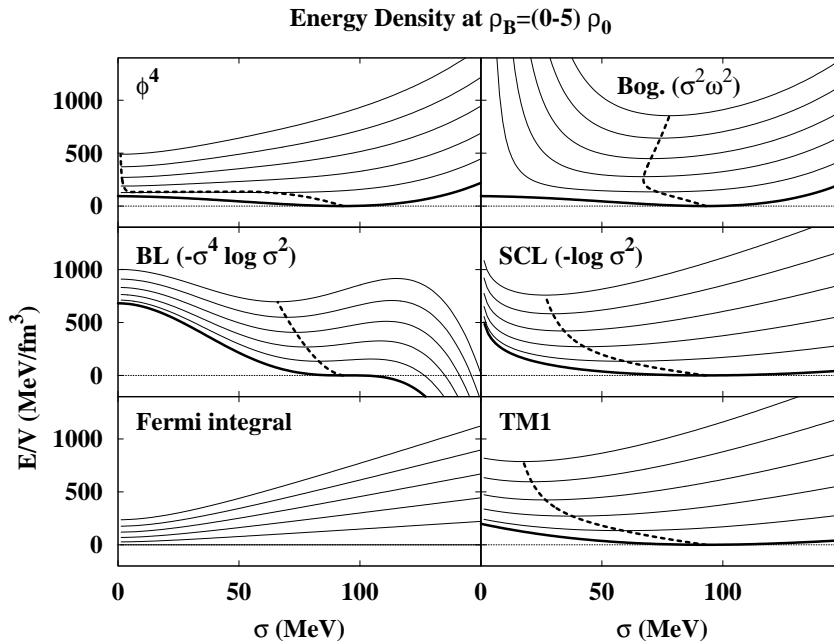


Fig. 3. Energy density at finite baryon densities. Calculated energy densities in vacuum (thick solid curves) and $\rho_B = (1-5)\rho_0$ (thin solid curves, from down to up as the density grows) as a function of σ are compared in chiral RMF models; the linear σ model (ϕ^4 , top left panel), the Boguta model (Bog., top right panel)^{18),24)}, the baryon loop model (BL, middle left panel)²⁰⁾, and the SCL model (middle right panel). The nucleon Fermi integral contribution (bottom left panel) and the results in the TM1 model (bottom right panel)¹⁰⁾ are also shown. The dotted curves show the equilibrium point where the energy density becomes the (local) minimum in the range of $\sigma < f_\pi$.

In Fig. 3, we compare the energy density as a function of σ at $\rho_B = (0-5)\rho_0$ in several RMF models. In the ϕ^4 model (left top panel), the nucleon Fermi integral contribution (left bottom panel in Fig. 3) is stronger than the repulsive potential at $\sigma < f_\pi$, and the vacuum collapses to the abnormal one at a density below ρ_0 .^{17)-19),24)} In order to avoid the chiral collapse, Boguta¹⁸⁾ replaced the vector meson mass term $m_\omega^2\omega^2/2$ with that of the $\sigma^2\omega^2$ coupling term,

$$\mathcal{L}_{\sigma\omega}^{\text{Boguta}} = \frac{1}{2} \frac{m_\omega^2}{f_\pi^2} \sigma^2 \omega^2. \quad (3.8)$$

In the case of no ω self-interactions, $c_\omega = 0$, the above coupling term gives large ω values at small σ as, $\omega = f_\pi^2 g_\omega \rho_B / m_\omega^2 \sigma^2$, leading to a strongly repulsive potential at finite densities. Because of this repulsion, nuclear matter EOS becomes stiff ($K > 600$ MeV), and σ increases again at around $\rho_B \simeq 0.27 \text{ fm}^{-3}$, as shown in the top right panel of Fig. 3.

In the left panel of Fig. 4, we compare the EOS in the present model with those in other RMF models. We adopt $m_\sigma = 502.63$ MeV, which fits bulk properties of finite nuclei and gives $K = 279.14$ MeV. Other parameters are summarized in

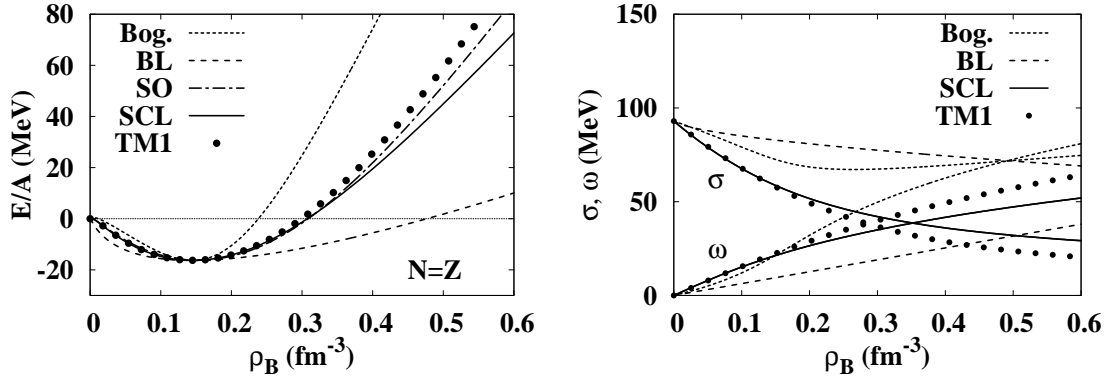


Fig. 4. Equation of state of symmetric nuclear matter (left panel) and density dependence of meson fields (right panel). We compare the calculated results in SCL (solid curves) with those in the Boguta (Bog., dotted curve)^{18),24)}, baryon loop (BL, dashed lines)²⁰⁾, Sahu-Ohnishi (SO, dot-dashed lines)²⁵⁾, and TM1 (filled circles)¹⁰⁾ models.

Table I. We find that the present model (SCL) gives softer EOS than that in the Boguta model (Bog.),^{18),24)} and its incompressibility is comparable to those in Sahu-Ohnishi (SO)²⁵⁾ and TM1¹⁰⁾ models. The baryon loop (BL) model²⁰⁾ gives the softest EOS in the models under consideration. However, it has instability at large σ values, and the incompressibility may be too small, $K \simeq 110$ MeV.

In addition to the similarity in EOS, σ and ω expectation values in the SCL model behave in a similar way to those in TM1 at low densities. In the right panel of Fig. 4, we show σ and ω expectation values as a function of ρ_B . We find that the σ expectation value decreases to around $\sigma \simeq 60$ MeV at $\rho_B \simeq \rho_0$ in the SCL and TM1 models, while the decrease is smaller in the BL and Boguta models.

The modifications of σ and ω from the vacuum values determine the nucleon scalar and vector(-isoscalar) potentials, $U_s(\rho_B) = -g_\sigma(f_\pi - \sigma)$ and $U_v(\rho_B) = g_\omega\omega$. TM models have been modeled to explain the bulk properties of nuclei such as the binding energies and nuclear radii, and these are mainly determined by the nuclear matter saturation properties and meson expectation values at around ρ_0 . Thus the above similarity of EOS and meson fields suggests that the SCL model could describe finite nuclei as the TM model.

3.2. Finite Nuclei

In describing finite nuclei, it is numerically preferable to use the shifted field, $\varphi \equiv f_\pi - \sigma$, since the boundary condition is given by $\varphi \rightarrow 0 (r \rightarrow \infty)$. We separate the σ mass term from the chiral potential V_σ as,

$$V_\sigma = \frac{1}{2}m_\sigma\varphi^2 + V_\varphi(\varphi), \quad V_\varphi(\varphi) = -2a_\sigma f_{\text{SCL}}\left(\frac{\varphi}{f_\pi}\right), \quad (3.9)$$

$$f_{\text{SCL}}(x) = \log(1-x) + x + \frac{x^2}{2}. \quad (3.10)$$

It is also necessary to include the photon field which represents the Coulomb potential. Here we take the static and mean-field approximation for boson fields, then RMF Lagrangian can be written as follows,

$$\begin{aligned} \mathcal{L}_X^{\text{RMF}} = & \bar{\psi}_N [i\cancel{\partial} - M_N^*(\varphi) - \gamma^0 U_v(\omega, R, A)] \psi_N - \frac{1}{2} (\nabla\varphi)^2 - \frac{1}{2} m_\sigma^2 \varphi^2 - V_\varphi(\varphi) \\ & + \frac{1}{2} (\nabla\omega)^2 + \frac{1}{2} m_\omega^2 \omega^2 + \frac{c_\omega}{4} \omega^4 + \frac{1}{2} (\nabla R)^2 + \frac{1}{2} m_\rho^2 R^2 + \frac{1}{2} (\nabla A)^2, \end{aligned} \quad (3.11)$$

$$M_N^*(\varphi) = M_N - g_\sigma \varphi, \quad U_v(\omega, R, A) = g_\omega \omega + g_\rho \tau_3 R + e \frac{1 + \tau_3}{2} A. \quad (3.12)$$

The field equations of motion derived from this Lagrangian read,

$$[-i\alpha \cdot \nabla + \beta M^* + U_v] \psi_N = \varepsilon_i \psi_N, \quad (3.13)$$

$$(-\Delta + m_\sigma^2) \varphi = g_\sigma \rho_S - \frac{dV_\varphi}{d\varphi}, \quad (3.14)$$

$$(-\Delta + m_\omega^2) \omega = g_\omega \rho_B - c_\omega \omega^3, \quad (3.15)$$

$$(-\Delta + m_\rho^2) R = g_\rho \rho_\tau, \quad (3.16)$$

$$-\Delta A = e \rho_B^p, \quad (3.17)$$

where $\rho_S = \rho_S^p + \rho_S^n$, $\rho_B = \rho_B^p + \rho_B^n$, $\rho_\tau = \rho_B^p - \rho_B^n$ denote scalar, baryon and isospin densities of nucleons, respectively. We solve the self-consistent coupled equations (3.13)-(3.17) by iteration until the convergence of total energy is achieved. In this work, we assume that nuclei are spherical, then the nucleon wave functions are expanded in spherical harmonic basis as follows,

$$\psi_{\alpha i \kappa m} = \begin{pmatrix} i[G_{i\kappa}^\alpha/r] \Phi_{\kappa m} \\ -[F_{i\kappa}^\alpha/r] \Phi_{-\kappa m} \end{pmatrix} \zeta_\alpha, \quad (3.18)$$

$$\rho_B^\alpha = \sum_i \left(\frac{n_{i\kappa\alpha}^{\text{occ}}}{4\pi r^2} \right) (|G_{i\kappa}^\alpha(r)|^2 + |F_{i\kappa}^\alpha(r)|^2), \quad (3.19)$$

$$\rho_S^\alpha = \sum_i \left(\frac{n_{i\kappa\alpha}^{\text{occ}}}{4\pi r^2} \right) (|G_{i\kappa}^\alpha(r)|^2 - |F_{i\kappa}^\alpha(r)|^2), \quad (3.20)$$

where ζ_α represents the isospin wave function (proton or neutron), $n_{i\kappa\alpha}^{\text{occ}}$ denotes the number of nucleons in that single particle level, and $\kappa = l$ and $-(l+1)$ for $j = l - 1/2$ and $j = l + 1/2$, respectively. Total energy is given by the integral of the energy density given as,

$$\begin{aligned} E = & \sum_{i,\kappa,\alpha} n_{i\kappa\alpha}^{\text{occ}} \varepsilon_{i\kappa\alpha} - \frac{1}{2} \int \{ -g_\sigma \varphi \rho_S + g_\omega \omega \rho_B + g_\rho R \rho_\tau + e^2 A \rho_B^p \} dr \\ & + \int \left(V_\varphi - \frac{1}{2} \varphi \frac{dV_\varphi}{d\varphi} + \frac{c_\omega}{4} \omega^4 \right) dr. \end{aligned} \quad (3.21)$$

We use Eqs. (3.13)-(3.17) to calculate second order derivatives of meson fields.

In comparing the calculated mean-field results with data, we have to take account of several corrections. In this work, we consider the center-of-mass (CM) correction

Parameters					
m_σ (MeV)	g_ω	g_ρ	c_ω		
502.63	13.02	4.40	200		
Constants					
M_N (MeV)	f_π (MeV)	m_π (MeV)	m_ω (MeV)	m_ρ (MeV)	$g_\sigma = M_N/f_\pi$
938	93	138	783	770	10.08
$\hbar c$ (MeV·fm)	ρ_0 (fm ⁻³)	$E/A(\rho_0)$ (MeV)	$\hbar\omega$ (MeV)	$\langle r_{\text{ch}}^2 \rangle_p$	$\langle r_{\text{ch}}^2 \rangle_n$
197.32705	0.145	-16.3	$41 A^{-1/3}$	$(0.862 \text{ fm})^2$	$-(0.336 \text{ fm})^2$

Table I. Parameters and constants adopted in the present work. Two of the parameters (g_ω and c_ω) are determined to fit the saturation point of symmetric nuclear matter and others (m_σ and g_ρ) are fixed through global fitting of Sn and Pb isotope binding energies.

and nucleon finite size correction in the same way as that adopted in Ref. 10). The CM kinetic energy is assumed to be

$$E_{\text{ZPE}} = \frac{\langle \mathbf{P}_{\text{CM}}^2 \rangle}{2AM_N} \simeq \frac{3}{4}\hbar\omega, \quad (3.22)$$

where $\mathbf{P}_{\text{CM}} = \sum_i \mathbf{p}_i$ is the CM momentum. This correction gives an exact result for harmonic-oscillator wave functions and we assume that it also applies to RMF wave functions. The CM correction on the proton rms radius is written as

$$\begin{aligned} \delta\langle r_p^2 \rangle &= -2\langle \mathbf{R}_{\text{CM}} \cdot \mathbf{R}_p \rangle + \langle \mathbf{R}_{\text{CM}}^2 \rangle \\ &\simeq \begin{cases} -\frac{3\hbar}{2AM_N\omega} & \text{(for heavy nuclei),} \\ -\frac{2Z}{A}\langle \mathbf{R}_p^2 \rangle + \langle \mathbf{R}_{\text{CM}}^2 \rangle = -\frac{2\langle r_p^2 \rangle}{A} + \frac{\langle r_M^2 \rangle}{A} & \text{(for light nuclei),} \end{cases} \end{aligned} \quad (3.23)$$

where $\mathbf{R}_p = \sum_{i \in p} \mathbf{r}_i/Z$ is the proton CM position, and $\langle r_p^2 \rangle$ and $\langle r_M^2 \rangle$ represent the proton and matter mean square radii, respectively. We assume again that harmonic-oscillator results applies for heavy nuclei. For light nuclei, we evaluate the correction in RMF wave functions, and we consider only the direct-term contributions. The charge rms radius is obtained by including the finite size effects of protons and neutrons,

$$\langle r_{\text{ch}}^2 \rangle = \langle r_p^2 \rangle + \langle r_{\text{ch}}^2 \rangle_p + \frac{N}{Z}\langle r_{\text{ch}}^2 \rangle_n, \quad (3.24)$$

We evaluate the binding energies and charge rms radii with these corrections, and the pairing energy for open-shell nuclei are neglected.

In describing finite nuclear properties, we have two free parameters, m_σ and g_ρ , which we cannot fix in nuclear matter. We have fitted the binding energies of Sn ($Z = 50$) and Pb ($Z = 82$) isotopes and have fixed the parameter values as $g_\rho = 4.40$ and $m_\sigma = 502.63$ MeV. Other parameters are obtained to fit the symmetric nuclear matter saturation point, and summarized in Table I. By using this parameter set, we have calculated the binding energies and charge rms radii of C to Pb isotopes.

B/A (MeV)										
Nucleus	exp.	SCL	TM1	TM2	NL1	NL3	I/110	IF/110	VIIIF/100	QMC-I
^{12}C	7.68	7.09	-	7.68	-	-	-	-	-	-
^{16}O	7.98	8.06	-	7.92	7.95	8.05	7.35	7.86	7.18	5.84
^{28}Si	8.45	8.02	-	8.47	8.25	-	-	-	-	-
^{40}Ca	8.55	8.57	8.62	8.48	8.56	8.55	7.96	8.35	7.91	7.36
^{48}Ca	8.67	8.62	8.65	8.70	8.60	8.65	-	-	-	7.26
^{58}Ni	8.73	8.54	8.64	-	8.70	8.68	-	-	-	-
^{90}Zr	8.71	8.69	8.71	-	8.71	8.70	-	-	-	7.79
^{116}Sn	8.52	8.51	8.53	-	8.52	8.51	-	-	-	-
^{196}Pb	7.87	7.87	7.87	-	7.89	-	-	-	-	-
^{208}Pb	7.87	7.87	7.87	-	7.89	7.88	7.33	7.54	7.44	7.25

charge rms radius (fm)										
Nucleus	exp.	SCL	TM1	TM2	NL1	NL3	I/110	IF/110	VIIIF/110	QMC-I
^{12}C	2.46	2.43	-	2.39	-	-	-	-	-	-
^{16}O	2.74	2.62	-	2.67	2.74	2.73	2.64	2.62	2.69	2.79
^{28}Si	3.09	3.04	-	3.07	3.03	-	-	-	-	-
^{40}Ca	3.45	3.44	3.44	3.50	3.48	3.47	3.41	3.40	3.45	3.48
^{48}Ca	3.45	3.46	3.45	3.50	3.44	3.47	-	-	-	3.52
^{58}Ni	3.77	3.77	3.76	-	3.73	3.74	-	-	-	-
^{90}Zr	4.26	4.27	4.27	-	4.27	4.29	-	-	-	4.27
^{116}Sn	4.63	4.62	4.61	-	4.61	4.61	-	-	-	-
^{196}Pb	-	5.48	5.47	-	5.47	-	-	-	-	-
^{208}Pb	5.50	5.54	5.53	-	5.57	5.58	5.49	5.49	5.53	5.49

Table II. Experimental and calculated binding energies and charge rms radii of stable nuclei. Calculated results in the SCL model are compared with those in TM1¹⁰⁾, TM2¹⁰⁾, NL1⁸⁾, NL3⁹⁾, glueball model (I/110)²⁷⁾, frozen glueball models (IF/110 and VIIIF/100)²⁷⁾, QMC-I³⁸⁾, and experimental data.

In Table II, we show the calculated results of binding energies per nucleon (B/A) and charge rms radii of doubly (sub-)closed stable nuclei, ^{12}C , ^{16}O , ^{28}Si , ^{40}Ca , ^{48}Ca , ^{58}Ni , ^{90}Zr , ^{116}Sn , ^{206}Pb and ^{208}Pb , in comparison with experimental data and other RMF model results. We find good overall agreement of the SCL results with experimental data for heavy nuclei. We underestimate B/A of several light nuclei, such as, ^{12}C , ^{28}Si and ^{58}Ni , by 0.2–0.6 MeV/ A . These nuclei have proton or neutron numbers of Z (or N) = 6, 14 and 28, *i.e.* they are jj closed nuclei. These underestimates imply that the spin-orbit interaction in the SCL model is not enough to explain the ℓs splittings in light nuclei. There are still discussions on the strength of the spin-orbit interactions in RMF,⁴⁴⁾ and it is recently suggested that the explicit role of pions has large effects in jj closed nuclei.^{45)–47)} Thus the underestimate may be related to the explicit pion effects.

In Fig. 5, we show B/A of C to Pb isotopes. We underestimate B/A in light jj closed nuclei and heavy Zr isotopes, the latter of which would be due to the deformation.^{10), 48)} Except for these nuclei, B/A are well explained in one parameter

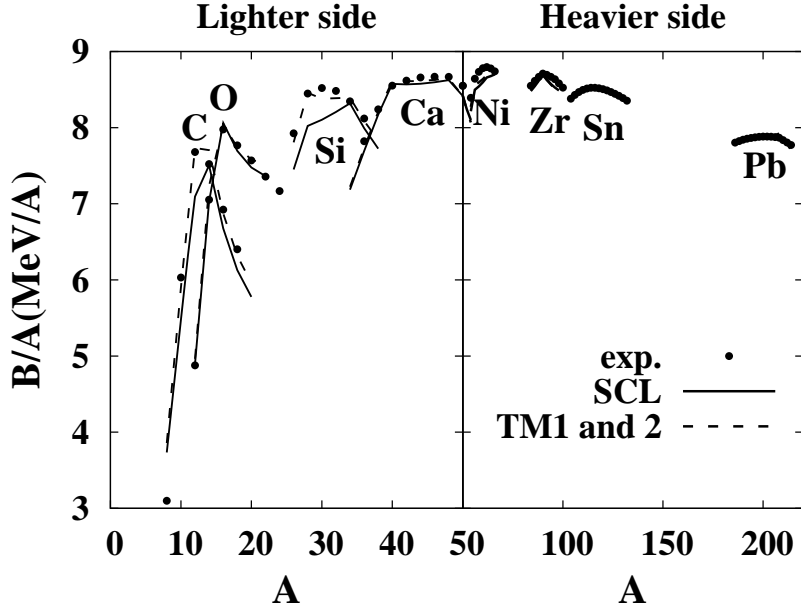


Fig. 5. Binding energies per nucleon of Z (sub-)closed nuclei. Calculated results in the SCL model (solid lines) are compared with experimental data (points) and TM^{10} models (dashed line).

set in the present SCL model. We also find that the SCL model results of B/A for heavy nuclei are very close to those in the $TM1$ model, where pairing corrections are neglected in $TM1$ model results. As shown in the top panel of Fig. 6, these two models give comparable results of nuclear densities. The agreement in the density distributions is not surprising since EOS and meson (σ and ω) behavior of SCL model is very similar to those in $TM1$ at low densities, as shown in Fig. 4. In the bottom panel of Fig. 6, we find some differences in the single particle energies, especially in those for neutrons around the Fermi energy.

There are several other chiral symmetric models well describing the nuclear matter as well as finite nuclei of ^{16}O , ^{40}Ca and ^{208}Pb .^(27),28) In these models, they introduce the broken scale invariance through the glueball field, and from scale invariance, this glueball is conjectured to couple with σ in a logarithmic term. In Ref. 27), Heide et al. proposed a chiral effective Lagrangian containing the glueball, and investigated nuclear matter and finite nuclear properties. With some of their parameter sets (I/110, IF/110), one can describe finite nuclear properties reasonably well, but these parameters give stiff nuclear matter EOS, $K > 340$ MeV. With the parameter set of VIIF, one can obtain reasonably soft EOS ($K = 267$ MeV), but the binding energies of nuclei are underestimated by $0.4 - 0.8$ MeV/A for ^{16}O , ^{40}Ca and ^{208}Pb . In Ref. 28), Furnstahl et al. extended the terms of the chiral effective Lagrangian with glueball having eight free parameters. In their work, the binding energies of ^{16}O , ^{40}Ca and ^{208}Pb nuclei are well described (up to 0.4 MeV/A deviation from the experimental data), and reasonably soft EOS's ($K = (194 - 244)$ MeV) are obtained. Compared to these models, the present SCL model describes nuclear

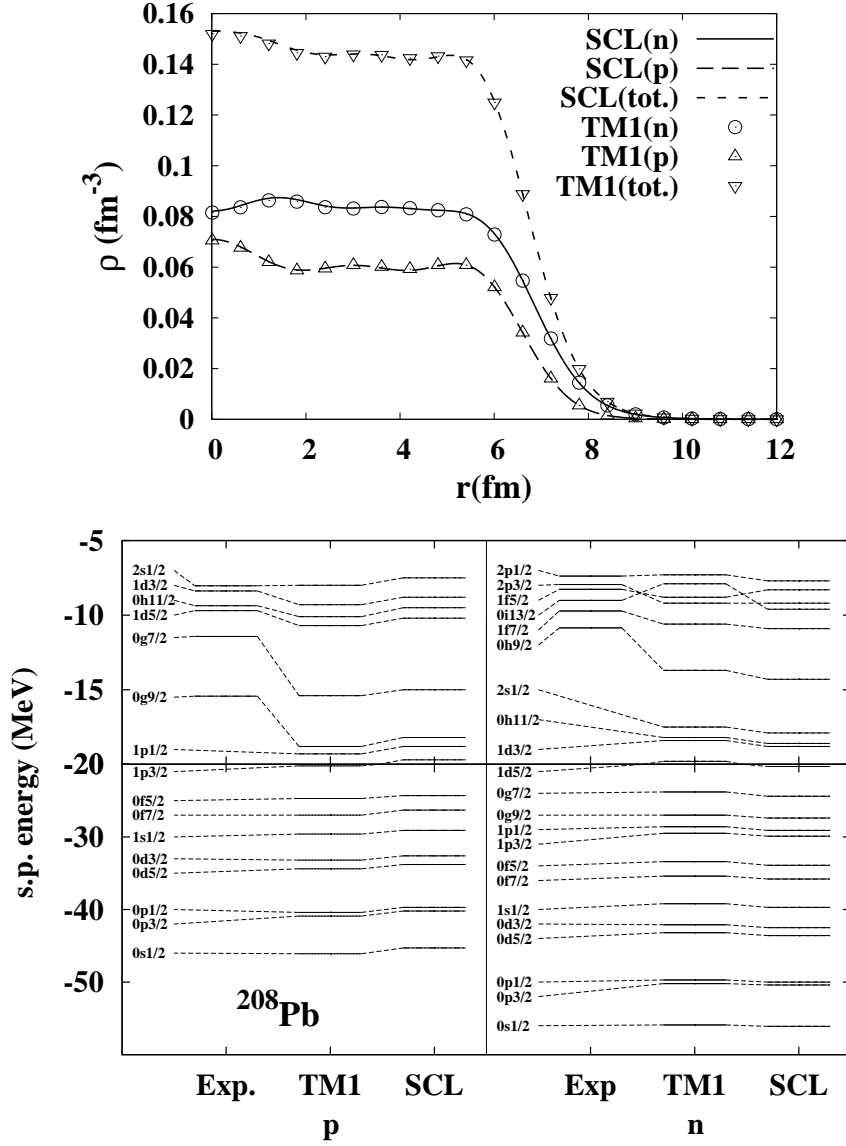


Fig. 6. Comparison of nuclear density (top) and single-particle energies (bottom) in the SCL and TM1¹⁰⁾ models for ^{208}Pb nucleus. Calculated results in SCL model are compared with those in TM1 model¹⁰⁾ and experimental data in Ref. 49).

matter and finite nuclei with only four free parameters. The main difference in the SCL model from these two glueball models may be in the ω self-interaction term, $c_\omega \omega^4$, simulating the suppression of ω at high densities in the Dirac-Brückner HF theory.¹¹⁾

§4. Naive dimensional analysis and scalar polarizability

The present SCL model is a kind of effective field theory and contains higher order terms and is non-renormalizable. Then it would be valuable to examine the naturalness in the naive dimensional analysis (NDA).^{29),40),43)} It is found that the loop contributions with the momentum cutoff $\Lambda \sim 1$ GeV generate the following terms with dimensionless coefficients C_{lmnp} of order unity,^{29),43)}

$$\mathcal{L}_{\text{int}} \sim \sum_{l,m,n,p} \frac{C_{lmnp}}{m!n!p!} \left(\frac{\bar{\psi}\Gamma\psi}{f_\pi^2\Lambda} \right)^l \left(\frac{\varphi}{f_\pi} \right)^m \left(\frac{\omega}{f_\pi} \right)^n \left(\frac{\rho}{f_\pi} \right)^p (f_\pi\Lambda)^2, \quad (4.1)$$

where Γ denotes the γ and $\tau/2$ when necessary.

An effective theory having terms in Eq. (4.1) is considered to hold naturalness, when all the dimensionless coefficients C_{lmnp} are of order unity. In the present SCL Lagrangian, we obtain the following dimensionless coefficients,

$$C_{1100} = \frac{f_\pi g_\sigma}{\Lambda} \sim 0.8, \quad C_{1010} = \frac{f_\pi g_\omega}{\Lambda} \sim 1.2, \quad C_{1001} = \frac{f_\pi g_\rho}{\Lambda} \sim 0.5, \quad (4.2)$$

$$C_{0n00} = \frac{(n-1)!(m_\sigma^2 - m_\pi^2)}{\Lambda^2} \sim 0.23, 1.4 \quad (n = 3, 4), \quad (4.3)$$

$$C_{0040} = \frac{6f_\pi^2 c_\omega}{\Lambda^2} \sim 10. \quad (4.4)$$

We find that the coefficients in the present SCL Lagrangian are natural except for higher order terms $\varphi^n (n \geq 5)$ and the phenomenological ω^4 term.

NDA is based on the assumption that internal gluon lines are suppressed by powers of $\alpha_s/4\pi$ ($\alpha_s = 0.28$),⁴³⁾ but it is not true in the strong coupling limit, where $\alpha_s = g_{\text{QCD}}^2/4\pi \rightarrow \infty$. For more serious evaluation of the model naturalness, therefore, it would be necessary to extend NDA to include gluon lines or to include the effects of finite coupling effects³⁶⁾ in the present SCL model.

It would be also valuable to examine the scalar polarizability in the SCL model. In the Quark Meson Coupling model (QMC)^{38),40)} and NJL model,³⁹⁾ non-linear coupling $\varphi^2\bar{\psi}\psi$ coming from the confinement is proposed to be essential to stabilize nuclear matter. This coupling gives nucleon mass curvature as a function of scalar condensate known as the scalar polarizability. We consider here the relation between SCL and QMC-I by redefining the σ fields as $\varphi = \tilde{\varphi} - \alpha\tilde{\varphi}^2$. With this redefinition, the non-linear coupling $\tilde{\varphi}^2\bar{\psi}\psi$ appears, and the sigma self-interaction term of order $\tilde{\varphi}^3$ disappears when we take $\alpha = 2a_\sigma/3f_\pi^3m_\sigma^2$,

$$\bar{\psi}(M_N - g_\sigma\varphi)\psi = \bar{\psi}(M_N - g_\sigma\tilde{\varphi} + \alpha g_\sigma\tilde{\varphi}^2)\psi, \quad (4.5)$$

$$V_\sigma = \frac{1}{2}m_\sigma^2\varphi^2 - 2a_\sigma f_{\text{SCL}}\left(\frac{\varphi}{f_\pi}\right) = \frac{1}{2}m_\sigma^2\tilde{\varphi}^2 + \mathcal{O}(\tilde{\varphi}^4). \quad (4.6)$$

Thus, except for the $\tilde{\varphi}^4$ term, we can map the SCL Lagrangian to QMC-I type having scalar polarizability in nuclear matter. The positive α value (positive curvature of nucleon mass) implies that the stabilization mechanism proposed in Refs.38), 39)

works also in this redefined Lagrangian. Quantitatively, the present polarizability parameter α is several times smaller than in QMC models,^{38),40)} and the σ kinetic term is modified by this redefinition. Therefore, the predictions are different as shown in Table II.

§5. Summary

In this work, we have developed a relativistic mean field (RMF) model with a chiral potential V_σ (vacuum energy density as a function of σ) having a logarithmic term derived in the strong coupling limit of the lattice QCD (SCL-LQCD).^{32)–37)} The logarithmic potential term of σ is found to have favorable features; it prevents the normal vacuum from collapsing, and it does not have any instabilities as a function of σ . We have introduced vector mesons (ω and ρ), their linear couplings to nucleons, and a non-linear vector meson self-interaction term $(\omega_\mu\omega^\mu)^2$ in a phenomenological way in order to fit the nuclear matter saturation point and the binding energies of finite nuclei. We have demonstrated that both of symmetric nuclear matter equation of state (EOS) and finite nuclear properties are well described in one parameter set containing four free parameters. The obtained EOS is comparable to those in successful but non-chiral models,^{9),10)} and to that in a chiral model containing higher order terms of σ .²⁵⁾ Binding energies of finite nuclei are also well reproduced in a wide mass range from C to Pb isotopes, while the binding energies of several light jj closed nuclei are underestimated, suggesting smaller spin-orbit interactions in the present model.

We compare the present SCL model with other RMF models in vacuum and finite densities in symmetric nuclear matter. We find that the baryon loop (BL)²⁰⁾ and Sahu-Ohnishi (SO)²⁵⁾ models have instability at large σ values, and the linear σ model with the $\sigma^2\omega^2$ coupling (Boguta model),^{18),24)} gives too stiff EOS. While the chiral RMF models with glueballs well describe both of nuclear matter and finite nuclei,^{26)–31)} introducing unobserved glueballs may not be justified in hadronic models. The energy functional in the present SCL model seems to be very similar to that in the TM1 model¹⁰⁾ at low densities. This point has been examined in the symmetric nuclear matter EOS and finite nuclear properties such as binding energies, charge rms radii, nuclear densities and single particle levels. At high densities, the SCL model gives a little softer EOS than that in TM1. This softness has some effects on neutron star properties and supernova explosion energies, which will be reported elsewhere.

Finally, we have performed a naive dimensional analysis (NDA),^{29),40),43)} and reinterpreted the SCL model in terms of the nucleon scalar polarizability.^{38)–40)} In NDA, we find that low dimension terms (mass dimension ≤ 4) in the SCL model are natural except for the ω^4 term. Since all the NDA analyses have been done without gluon lines, it is necessary to take account of finite coupling corrections in NDA⁴³⁾ or in SCL³⁶⁾ for serious evaluation of the naturalness. By using the field redefinition, $\varphi = \tilde{\varphi} - \alpha\tilde{\varphi}^2$, we can relate the SCL model Lagrangian to that having nucleon scalar polarizability such as QMC-I,³⁸⁾ while the polarizability is a few times smaller than those in QMC models.^{38),40)}

There are several directions to be investigated further. First, the binding energy underestimate problem in jj closed light nuclei should be studied in an extended framework including explicit role of pions.^{45),46)} Next, it is desirable to extend the present model to that with flavor SU(3) chiral symmetry. Preliminary works suggest that we can obtain a softer EOS ($K \simeq 210$ MeV) due to the coupling of sigma meson to hidden strangeness.⁵⁰⁾ Thirdly, it is interesting to take account of the finite temperature effects in the chiral potential V_σ . It has been shown that V_σ is smoothed at finite temperature around $\sigma \sim 0$ in SCL-LQCD,³³⁾⁻³⁶⁾ then it may be possible to describe chiral phase transitions from nuclear matter to quark matter at high temperatures in chiral RMF models.

Acknowledgments

We would like to thank Dr. K. Naito for important discussions in the initial stage of this work. This work is supported in part by the Ministry of Education, Science, Sports and Culture, Grant-in-Aid for Scientific Research under the grant numbers, 15540243 and 1707005.

References

- 1) H. Yukawa, Proc. Phys. Math. Soc. Japan **17** (1935), 48.
- 2) M. Gell-Mann and M. Levy, Nuovo Cimento **16** (1960), 705.
- 3) Y. Nambu and G. Jona-Lasino, Phys. Rev. **122** (1961), 345; Phys. Rev. **124** (1961), 246.
- 4) T. Hatsuda and T. Kunihiro, Phys. Rept. **247** (1994), 221 [arXiv:hep-ph/9401310].
- 5) S. Weinberg, Gravitation and Cosmology: Principles and Applications of the General Theory of Relativity (John Wiley & Sons, New York, 1972); J. Gasser and H. Lertwylter, Ann. Phys. **158** (1984), 142; Nucl. Phys. B **250** (1985), 465.
- 6) B. D. Serot and J. D. Walecka, Adv. in Nucl. Phys. **16** (1986), 1.
- 7) J. Boguta and A. R. Bodmer, Nucl. Phys. A **292** (1977), 413.
- 8) P. -G. Reinhard, M. Rufa, J. Maruhn, W. Greiner and J. Friedrich, Z. Phys. A **323** (1986), 13; Suk-Joon Lee, J. Fink, A. B. Valantekin, M. R. Strayer, A. S. Umar, P. G. Reinhard, J. A. Maruhn and W. Greiner, Phys. Rev. Lett. **57** (1986), 2916.
- 9) G.A. Lalazissis, J. König and P. Ring, Phys. Rev. C **55** (1997), 540 [arXiv:nucl-th/9607039].
- 10) Y. Sugahara and H. Toki, Nucl. Phys. A **579** (1994), 557.
- 11) R. Brockmann and H. Toki, Phys. Rev. Lett. **68** (1992), 3408.
- 12) B. C. Clark, S. Hama, R. L. Mercer, L. Ray and B. D. Serot, Phys. Rev. Lett. **50** (1983), 1644
- 13) H. Shen, H. Toki, K. Oyamatsu and K. Sumiyoshi, Prog. Theor. Phys. **100** (1998), 5 [arXiv:nucl-th/9806095].
- 14) K. Sumiyoshi, H. Suzuki, S. Yamada and H. Toki, Nucl. Phys. A **730** (2004), 227 [arXiv:nucl-th/0310046].
- 15) C. Ishizuka, A. Ohnishi and K. Sumiyoshi, Nucl. Phys. A **723** (2003), 517 [arXiv:nucl-th/0208020].
- 16) A. W. Thomas, P. A. M. Guichon, D. B. Leinweber and R. D. Young, Prog. Theor. Phys. Suppl. **156** (2004), 124 [arXiv:nucl-th/0411014].
- 17) T. D. Lee and G. C. Wick, Phys. Rev. D **9** (1974), 2291.
- 18) J. Boguta, Phys. Lett. B **120** (1983), 34; Phys. Lett. B **128** (1983), 19.
- 19) T. D. Lee and M. Margulies, Phys. Rev. D **11** (1975), 1591.
- 20) T. Matsui and B. D. Serot, Ann. Phys. (N.Y.) **144** (1982), 107.
- 21) T. Hatsuda and M. Prakash, Phys. Lett. B **224** (1989), 11.
- 22) L. G. Liu, W. Bentz and A. Arima, Ann. Phys. **194** (1989), 387.
- 23) S. Tamenaga, H. Toki, A. Haga and Y. Ogawa, arXiv:nucl-th/0604013.

- 24) Y. Ogawa, H. Toki, S. Tamenaga, H. Shen, A. Hosaka, S. Sugimoto and K. Ikeda, *Prog. Theor. Phys.* **111** (2004), 75 [arXiv:nucl-th/0312042].
- 25) P. Sahu and A. Ohnishi, *Prog. Theor. Phys.* **104** (2000), 1163 [arXiv:nucl-th/0007068].
- 26) R. J. Furnstahl and B. D. Serot, *Phys. Lett. B* **316** (1993), 12.
- 27) E. K. Heide, S. Rudaz, and P. J. Ellis, *Nucl. Phys.* **A571** (1994), 713 [arXiv:nucl-th/9308002].
- 28) R. J. Furnstahl, H. B. Tang, and B. D. Serot, *Phys. Rev. C* **52** (1995), 1368 [arXiv:hep-ph/9501386].
- 29) R. J. Furnstahl, B. D. Serot and H. B. Tang, *Nucl. Phys. A* **615** (1997), 441 [Erratum-ibid. *A* **640** (1998), 505] [arXiv:nucl-th/9608035].
- 30) I. Mishustin, J. Bondorf, and M. Rho, *Nucl. Phys.* **A555** (1993), 215.
- 31) P. Papazoglou, J. Schaffner, S. Schramm, D. Zschesche, H. Stöcker, and W. Greiner, *Phys. Rev. C* **55** (1997), 1499 [arXiv:nucl-th/9609035]; P. Papazoglou, S. Schramm, J. Schaffner-Bielich, H. Stöcker, and W. Greiner, *Phys. Rev. C* **57** (1998), 2576 [arXiv:nucl-th/9706024].
- 32) N. Kawamoto and J. Smit, *Nucl. Phys. B* **190** (1981), 100.
- 33) N. Kawamoto, K. Miura, A. Ohnishi and T. Ohnuma, *Phys. Rev. D* **75** (2007), 014502 [arXiv:hep-lat/0512023].
- 34) Y. Nishida, *Phys. Rev. D* **69** (2004), 094501 [arXiv:hep-ph/0312371].
- 35) P. H. Damgaard, N. Kawamoto and K. Shigemoto, *Phys. Rev. Lett.* **53** (1984), 2211; E. M. Ilgenfritz and J. Kripfganz, *Z. Phys. C* **29** (1985), 79; P. H. Damgaard, N. Kawamoto and K. Shigemoto, *Nucl. Phys. B* **264** (1986), 1; N. Bilic, K. Demeterfi and B. Petersson, *Nucl. Phys. B* **377** (1992), 651; Y. Nishida, K. Fukushima and T. Hatsuda, *Phys. Rept.* **398** (2004), 281 [arXiv:hep-ph/0306066]; X. Q. Luo, *Phys. Rev. D* **70** (2004), 091504(R) [arXiv:hep-lat/0405019].
- 36) G. Faldt and B. Petersson, *Nucl. Phys. B* **265** (1986), 197; N. Bilic, F. Karsch and K. Redlich, *Phys. Rev. D* **45** (1992), 3228; N. Bilic and J. Cleymans, *Phys. Lett. B* **355** (1995), 266 [arXiv:hep-lat/9501019]; A. Ohnishi, N. Kawamoto and K. Miura, *J. Phys. G*, to appear [arXiv:hep-lat/0701024].
- 37) N. Kawamoto, *Nucl. Phys. B* **190** (1981), 617; J. Hoek, N. Kawamoto and J. Smit, *Nucl. Phys. B* **199** (1982), 495; H. Kluberg-Stern, A. Morel and B. Petersson, *Nucl. Phys. B* **215** (1983), 527; P. H. Damgaard, D. Hochberg and N. Kawamoto, *Phys. Lett. B* **158** (1985), 239; E. Dagotto, F. Karsch and A. Moreo, *Phys. Lett. B* **169** (1986), 421; F. Karsch and K. H. Mutter, *Nucl. Phys. B* **313** (1989), 541; J. U. Klatke and K. H. Mutter, *Nucl. Phys. B* **342** (1990), 764; V. Azcoiti, G. Di Carlo, A. Galante and V. Laliena, *J. High Energy Phys.* **0309** (2003), 014 [arXiv:hep-lat/0307019]; K. Fukushima, *Prog. Theor. Phys. Suppl.* **153** (2004), 204 [arXiv:hep-ph/0312057].
- 38) K. Saito, K. Tsushima and A. W. Thomas, *Phys. Rev. C* **55** (1997), 2637 [arXiv:nucl-th/9612001].
- 39) W. Bentz and A. W. Thomas, *Nucl. Phys. A* **696** (2001), 138 [arXiv:nucl-th/0105022].
- 40) K. Saito, K. Tsushima and A. W. Thomas, *Phys. Lett. B* **406** (1997), 287 [arXiv:nucl-th/9704047].
- 41) C. DeTar and T. Kunihiro, *Phys. Rev. D* **39** (1989), 2805.
- 42) M. Harada and K. Yamawaki, *Phys. Rev. Lett.* **86** (2001), 757.
- 43) A. Manohar and H. Georgi, *Nucl. Phys. B* **234** (1984), 189; H. Georgi and L. Randall, *Nucl. Phys. B* **276** (1986), 241; H. Georgi, *Phys. Lett. B* **298** (1993), 187 [arXiv:hep-ph/9207278].
- 44) A. Bhagwat, R. Wyss, W. Satula, J. Meng and Y. K. Gambhir, arXiv:nucl-th/0605009.
- 45) K. Ikeda, S. Sugimoto and H. Toki, *Nucl. Phys. A* **738** (2004), 73 [arXiv:nucl-th/0402075].
- 46) A. Isshiki, A. Ohnishi and K. Naito, *Prog. Theor. Phys.* **114** (2005), 573 [arXiv:nucl-th/0407085].
- 47) A. Bouyssy, J. F. Mathiot, V. G. Nguyen and S. Marcos, *Phys. Rev. C* **36** (1987), 380.
- 48) D. Hirata, K. Sumiyoshi, I. Tanihata, Y. Sugahara, T. Tachibana and H. Toki, *Nucl. Phys. A* **616** (1997), 438.
- 49) D. Vautherin and D. M. Brink, *Phys. Rev. C* **5** (1972), 626.
- 50) K. Tsubakihara, H. Maekawa, A. Ohnishi, *Proc. of IX Int. Conf. on Hypernuclear and Strange Particle Physics*, Mainz, Germany, Oct. 10-14, 2006, *Euro. Phys. J. A*, to appear [arXiv:nucl-th/0702008].